Title

Co-occurring mutations of tumor suppressor genes, *LATS2* and *NF2*, in malignant pleural mesothelioma

Authors and affiliations

1. Robin Tranchant[1,2,3,4]
2. Lisa Quetel[1,2,3,4]
3. Anne Tallet[1,*]
4. Clement Meiller[1,2,3,4]
5. Annie Renier[1,2,3,4]
6. Leanne De Koning[5]
7. Aurélien de Reyniès[6]
8. Francoise Le Pimpec-Barthes[1,2,3,4,7,8]
9. Jessica Zucman-Rossi[1,2,3,4,8]
10. Marie-Claude Jaurand[1,2,3,4]
11. Didier Jean[1,2,3,4]

[1]Inserm, UMR-1162, Génomique fonctionnelle des tumeurs solides, Equipe labellisée Ligue Contre le Cancer, F-75010, Paris, France.
[2]Université Paris Descartes, Sorbonne Paris Cité, Labex Immuno-oncology, F-75000, Paris, France.
[3]Université Paris Diderot, Sorbonne Paris Cité, Institut Universitaire d'Hématologie, Paris, F-75010, France.
[4]Université Paris 13, Sorbonne Paris Cité, F-93206, Saint-Denis, France.
[5]Institut Curie, PSL Research University, Translational Research Department, F-75005, Paris, France.
[6]Programme Cartes d'Identité des Tumeurs (CIT), Ligue Nationale Contre Le Cancer, F-75013, Paris, France.
[7]Département de Chirurgie Thoracique, Hôpital Européen Georges Pompidou, F-75015, Paris, France.
[8]Assistance Publique-Hôpitaux de Paris, Hôpital Européen Georges Pompidou, F-75015, Paris, France.
* Present address: Platform of Somatic Tumor Molecular Genetics, University Hospital, F-37000, Tours, France

Conflicts of Interest

The authors declare no potential conflicts of interest.

Running title

LATS2/NF2 co-occurring mutations in mesothelioma

Keywords

Thoracic tumor - Tumor molecular classification - Co-occurring genetic alterations - Signal pathway – Target therapy

Word count

4998

Total number of figures and tables

5 figures + 1 table

Grant support

This work was supported by INSERM, the Fondation ARC pour la recherche sur le cancer, the Ligue Contre le Cancer (Ile de France and Oise committees), the Groupement des Entreprises Françaises dans la Lutte contre le Cancer (GEFLUC), and the Chancellerie des Universités de Paris (Legs POIX).

Corresponding author

Didier JEAN
INSERM UMR-1162
27, rue Juliette Dodu
F-75010 PARIS
FRANCE
Phone: +33 (0)1 72 63 93 50
E-mail address: didier.jean@inserm.fr

Disclosure of Potential Conflicts of Interest

No potential conflicts of interest were disclosed.

Authors' Contributions

Conception and design:

R. Tranchant, F. Le Pimpec-Barthes, J. Zucman-Rossi, M.C. Jaurand, D. Jean.

Development of methodology:

R. Tranchant, A. Renier, C. Meiller, A. Tallet.

Acquisition of data:

R. Tranchant, L. Quetel, A. Tallet, A. Renier, L. de Koning

Analysis and interpretation of data:

R. Tranchant, A. de Reynies, M.C. Jaurand, D. Jean.

Writing, review and/or revision of the manuscript:

R. Tranchant, M.C. Jaurand, D. Jean.

Administrative, technical or material support:

A. Renier, C. Meiller, F. Le Pimpec-Barthes

Study supervision:

J. Zucman-Rossi, M.C. Jaurand, D. Jean.

Acknowledgments

The authors thank the members of the IUH technological platform for their help with flow cytometry (Niclas Setterblad, Christelle Doliger and Sophie Duchez), the Institut Curie RPPA platform for acquisition of RPPA data (Aurélie Cartier, Bérengère Ouine and Audrey Criqui) and the Institut Curie bioinformatics platform for bioinformatics support (Patrick Poullet, Stéphane Liva and Philippe Hupé).

Translational Relevance

Malignant pleural mesothelioma (MPM) is a devastating therapy-resistant cancer. Knowledge of the molecular alterations and clinico-biological heterogeneity involved is critical to improve MPM therapeutic efficiency. We recently established a robust molecular MPM classification consisting of two groups characterized by different molecular profiles and survival outcomes. In the present study, we defined a new homogeneous tumor subgroup that shares common genetic alterations and similar gene expression profiles. Characterization of specific deregulated signal pathways led us to identify an anticancer compound, an inhibitor of the mTOR/PI3K/AKT pathway already used in clinical trials for other types of cancer, to target this MPM subgroup. To better select patients eligible for this targeted therapy, we also proposed a potential biomarker. Our findings highlight the importance for translational research of taking genetic alteration, transcriptomic classification and signal pathway activation into account to establish a new therapeutic approach and to improve MPM management.

Abstract

PURPOSE: To better define MPM heterogeneity and identify molecular subtypes of malignant pleural mesothelioma (MPM), we focus on the tumor suppressor gene *LATS2*, a member of the Hippo signaling pathway, which plays a key role in mesothelial carcinogenesis.

EXPERIMENTAL DESIGN: Sixty-one MPM primary cultures established in our laboratory were screened for mutations in *LATS2*. Gene inactivation was modeled using siRNAs. Gene and protein expressions were analyzed by quantitative RT-PCR, western blot and RPPA. Cell proliferation, viability, apoptosis, mobility and invasion were determined after siRNA knockdown or YAP (verteporfin), mTOR (rapamycin) and mTOR/PI3K/AKT (PF_04691502) inhibitor treatment.

RESULTS: The *LATS2* gene was altered in 11% of MPM by point mutations and large exon deletions. Genetic data coupled with transcriptomic data allowed the identification of a new MPM molecular subgroup, $C2^{LN}$, characterized by a co-occurring mutation in the *LATS2* and *NF2* genes in the same MPM. MPM patients of this subgroup presented a poor prognosis. Co-inactivation of *LATS2* and *NF2* leads to loss of cell contact inhibition between MPM cells. Hippo signaling pathway activity, mTOR expression and phosphorylation were altered in the $C2^{LN}$ MPM subgroup. MPM of this new subgroup show higher sensitivity to PF_04691502 inhibitor. The *MOK* gene was identified as a potential biomarker of the $C2^{LN}$ MPM subgroup and PF_04691502 sensitivity.

CONCLUSIONS: We identified a new MPM molecular subgroup that shares common genetic and transcriptomic characteristics. Our results made it possible to highlight a greater sensitivity to an anticancer compound for this MPM subgroup and to identify a specific potential biomarker.

Introduction

Malignant pleural mesothelioma (MPM) is an aggressive tumor that is resistant to conventional anticancer therapies (surgery, radiotherapy and chemotherapy), resulting in poor prognosis and very short patient survival (an average of 12 months). Its major risk factor is past exposure to asbestos fibers, a carcinogen that induces genomic and genetic alterations (1). To improve the prognosis of this disease, there is a strong need to develop efficient therapeutic strategies, taking the molecular alterations and clinico-biological heterogeneity of tumors into account.

MPM is characterized by numerous chromosomal abnormalities, gene mutations (mainly deletions), epigenetic alterations and specific gene expression (2). Heterogeneity of tumors was found at these different molecular levels. Concerning the genetic alteration, sequencing analyses showed that alterations mostly concern tumor suppressor genes. Mutations in *CDKN2A* (Cyclin-dependent kinase inhibitor 2A), *CDKN2B* (Cyclin-dependent kinase inhibitor 2B), *BAP1* (BRCA1 associated protein-1) and *NF2* (Neurofibromin 2) have been reported in a high percentage of MPM. Mutations in *TP53* (Tumor protein p53) were also found but at a lower percentage (3). Recent next-generation sequencing studies did not find any frequent recurrent alterations in other tumor suppressor genes or oncogenes (4-6). A recurrent oncogenic mutation in the *TERT* promoter was previously found in our laboratory. It was the first hotspot oncogenic mutation identified in MPM (7).

We previously defined a robust MPM molecular classification consisting of two groups (C1 and C2) with different molecular profiles, gene alterations, histology subtypes and survival outcomes. Epithelioid MPM were found in both groups with a worse survival prognosis in the C2 group. The C1 group exhibited more frequent *BAP1* alterations and the C2 group presented a mesenchymal phenotype (8).

The Hippo signaling pathway plays a key role in the control of organ size and in carcinogenesis by regulating cell growth and apoptosis (9). The Hippo pathway regulates the transcriptional co-activator YAP (Yes-associated protein, *YAP1* gene) activity, which is involved in MPM carcinogenesis (10, 11). Under healthy conditions, at high cell density, YAP is phosphorylated and sequestrated in the cytoplasm after interaction with 14-3-3 proteins, resulting in proteasomal degradation. At low cell density, YAP is transduced to the nucleus and interacts with several transcription factors, including TEAD family members, to promote expression of target genes that promote carcinogenesis (12). In MPM, recurrent inactivating mutations are found in members of this pathway, *NF2* and *LATS2* (large tumor suppressor 2) genes, resulting in aberrant co-transcriptional activity of YAP. However, the alteration frequency of *LATS2* in MPM remains unclear (6, 13, 14).

In the present study, we first focused on *LATS2* gene alteration on our collection of MPM primary cultures to better define the frequency and the mechanism of *LATS2* inactivation in MPM. Based on genetic alterations and transcriptomic classification, we identified a specific MPM molecular subgroup characterized by a co-occurring mutation in *LATS2* and *NF2*. Molecular analysis makes it possible to identify specific signal pathways deregulated in this MPM subgroup. These data allowed us to identify a specific biomarker and to highlight a greater sensitivity to an anticancer compound for this MPM subgroup.

Materials and Methods

Mesothelioma cells in culture

MPM in culture (61 cases), previously characterized for genetic alterations in key genes of mesothelial carcinogenesis (*CDKN2A*, *CDKN2B*, *BAP1*, *NF2* and *TP53*), were primary cell lines established in our laboratory (they can therefore not be authenticated) and used in several previous studies showing their relevance to MPM primary tumors (7, 8, 15, 16). Clinico-pathological, epidemiologic and molecular data are reported in Table 1.

siRNA-targeted knockdown

RNA interference was used to knockdown *NF2*, *LATS2* and *YAP* expression in MPM cells by using two different siRNA for each targeted gene. Silencer Select pre-designed siRNA were purchased from Thermo Fisher Scientific/Ambion (Supplementary Table S1). Knockdown was performed by reverse transfection of siRNA into cells using Lipofectamine RNAiMAX reagent (Thermo Fisher Scientific) according to the manufacturer's instructions. Briefly, 3.10^5 cells were seeded on 6-well plates (TPP) and transiently transfected with equal amounts of siRNA (4 nM siRNA for simple transfection and 8 nM for co-transfection), using 2.5 µl/mL of transfection reagent. As a control, cells were transfected without siRNA and with two untargeting siRNA (Silencer Select Negative Control #1 or #2 siRNA, Thermo Fisher Scientific/Ambion).

Cell proliferation and inhibitor assays

For proliferation, MPM cells were seeded in triplicate and transfected on 96-well plates (Corning, Falcon) at different concentrations: 5.10^3 or 1.10^4 cells/well for non-confluent conditions and 3.10^4 cells/well for confluent conditions. For inhibitor assays, MPM cells were

seeded at 1.10^4 cells/well in triplicate. Cells were treated for 48 hours with gradient concentrations of a potent YAP inhibitor (verteporfin; #S1786; Selleck Chemicals), a specific mTOR inhibitor (rapamycin; #S1039; Selleck Chemicals) or a specific mTOR/PI3K/Akt inhibitor (PF-04691502; #S2743; Selleck Chemicals). Cell proliferation was quantified by MTS assay (CellTiter 96 AQueous One Solution Cell Proliferation Assay, Promega) using an absorbance reader (FLUOstar Omega, BMG Labtechnologies). Area Under Curve (AUC) was determined by Graph Pad Prism 6 software for inhibitor assays. Results were obtained from at least two independent experiments. Apoptosis assays were performed by Annexin V and propidium iodide (PI) staining (see Supplementary Methods for details)

Mutation and gene expression analysis

Genetic alterations in the *LATS2* gene in MPM cells were screened by Sanger sequencing as previously described (7, 16), using specific primers (Supplementary Table S2). Gene expression was analyzed by quantitative RT-PCR. Protein expression was determined by Western blot and Reverse Protein Phase Array (RPPA) technology (see Supplementary Methods for details). RPPA was performed on 39 MPM in culture as previously described (17) and arrays revealed with the antibodies are given in Supplementary Table S3. Raw data were normalized using NormaCurve, which normalizes for fluorescent background per spot and a total protein stain (18).

Statistical analyses

Unsupervised consensus clustering analysis of the 23 MPM of the C2 subgroup was performed using Affymetrix HG-U133-plus-2.0 microarray data (ArrayExpress accession number E-MTAB-1719) as previously reported (8). Differentially expressed genes were identified from microarray data using the Bioconductor Limma package in the statistical

program R (19). Graph Pad Prism version 6 software was used to perform the other statistical tests: Mann–Whitney test for the whole MPM series data, t test for the siRNA experiment and log-rank test of the Kaplan–Meier plot for survival comparison. *P*-values are shown in the figure as * $P < 0.05$, ** $P < 0.01$ and *** $P < 0.001$.

Results

Genetic alterations in the *LATS2* gene

Genetic alterations in the *LATS2* gene were studied by DNA sequence analysis using our series of 61 MPM in culture (Table 1). *LATS2* mutations were detected in seven of the 61 MPM in culture (11%) and consisted of three large deletions and four different point mutations (Fig. 1A and Supplementary Table S4). MPM_18 and MPM_40 showed a deletion of exon 2, and MPM_29 showed a deletion of exons 3 and 4. Two nonsense mutations were found in exon 4 of MPM_08 (c.1237C>T, p.Q413*) and MPM_14 (c.685C>T, p.Q229*). A frameshift mutation introduced a stop codon in exon 5 (c.1425delC, p.P475fs) into MPM_47. One missense mutation c.2873G>A (p.R958H) was found in exon 8 (coding for the catalytic kinase domain of the LATS2 protein) of MPM_04 with functional consequences on the protein activity, according to prediction programs. None of these mutations was previously identified in the COSMIC database (http://cancer.sanger.ac.uk/cosmic/; last access: November 16, 2016). MPM without mutation expressed *LATS2* mRNA and LATS2 protein (Fig. 1B-C). Complete loss of mRNA expression was only observed in MPM with large exon deletions (Fig. 1B). Among the seven *LATS2* mutants, only the MPM in culture with missense mutation (MPM_04) showed LATS2 protein expression (Fig. 1C).

Molecular characteristics of *LATS2* MPM mutants are shown in Fig. 1D. Mutants were mainly found in the C2 molecular tumor group (6/7 cases). No significant association was found between *LATS2* mutations and genetic alterations in other genes involved in mesothelial carcinogenesis (*CDKN2A*, *CDKN2B*, *BAP1*, *NF2* and *TP53*). Interestingly, five of the seven *LATS2* mutants (8% of all the MPM) are also mutated for *NF2*, another member of the Hippo signaling pathway, which is otherwise altered in 27 MPM in culture (44%). We focused on these MPM with *LATS2*/*NF2* co-occurring mutations, all found in the C2 molecular group.

Molecular subgroup of MPM with *LATS2/NF2* co-occurring mutations

Three MPM with *LATS2*/*NF2* co-occurring mutations (MPM_04, MPM_08 and MPM_29) were part of a previous transcriptomic analysis (8). In the present study, we performed an unsupervised consensus classification of the C2 group (Fig. 2A). The three MPM with co-occurring mutations were found in a C2 subgroup and shared similar transcriptomic profiles with two other MPM (MPM_18 and MPM_38). MPM_18 is only mutated in *LATS2* gene and MPM_38 is wild-type for both *LATS2* and *NF2*. As it is known *WWTR1* (encoding the TAZ transcription coactivator closely related to YAP (12)) may play a role in the function of the Hippo pathway, gene expression of both *YAP1* and *WWTR1* was analyzed in the MPM series. MPM in culture have a relatively homogeneous expression for both genes except MPM_38, which is characterized by a strong overexpression of *WWTR1* gene (Supplementary Fig. S1). This subgroup of five MPM is further referred to as $C2^{LN}$. The two MPM with *LATS2*/*NF2* co-occurring mutations (MPM_47 and MPM_40) that were not included in the transcriptomic analysis but classified in the C2 group using gene predictors (8) were integrated into the $C2^{LN}$ MPM subgroup for the subsequent analyses.

Among the MPM in the $C2^{LN}$ subgroup, three were sarcomatoid, two epithelioid and one biphasic. No significant difference was found between the $C2^{LN}$ MPM subgroup and other MPM patients concerning gender, age or asbestos exposure. Overall survival of the $C2^{LN}$ subgroup of MPM patients was lower compared to overall *NF2*-mutated MPM and other MPM patients (P=0.02) (Fig. 2B).

Effect of *LATS2/NF2* co-inactivation on proliferation, invasion and migration of MPM cells

Simple or double inactivation of *LATS2* and *NF2* was simulated in three different MPM wild-type cells for *LATS2* and *NF2* genes (MMP_07, MMP_32 and MPM_34) using efficient siRNA (Supplementary Fig. S2). Cell proliferation was measured in si*LATS2* and/or si*NF2* transfected cells and compared to siControl transfected cells. A significant increase of proliferation in MPM_34 cells transfected with si*LATS2*/*NF2* was observed only when the cells reached the confluent state (Fig. 2C). Consistently, in the three MPM cells transfected with si*LATS2*/*NF2*, no effect was observed up to a confluent state (Supplementary Fig. S3A) but a proliferation increase of 30 to 50% was found at confluence (Fig. 2D). In agreement with these observations, foci formation was observed when MPM of the $C2^{LN}$ subgroup were maintained at confluence (Supplementary Fig. S3B). After single inactivation of *LATS2* or *NF2*, a slight increase was observed in only two MPM in culture (around 20% for MPM_07 and MPM_32) with *LATS2* siRNA, and no effect on proliferation was observed with *NF2* siRNA (Fig. 2D). Inactivation by siRNA of both *LATS2* and *NF2* did not modify cell migration or invasion (Supplementary Fig. S3C-D).

Pathway deregulation of the $C2^{LN}$ subgroup MPM

To explore signaling pathways impaired by *LATS2*/*NF2* co-occurring mutations, we compared phosphorylation levels of 40 proteins, key members of several major signaling pathways, between the $C2^{LN}$ MPM subgroup and the other MPM by RPPA (Supplementary Table S3). The phosphorylation level was significantly decreased in the $C2^{LN}$ MPM subgroup for YAP, the serine/threonine protein kinase mTOR (mammalian target of rapamycin) and the EPHA2 receptor tyrosine factor in the $C2^{LN}$ MPM subgroup (Fig. 3A and Supplementary Fig. S4A-B).

To validate the decrease of YAP phosphorylation in MPM of the $C2^{LN}$ subgroup, we studied YAP phosphorylation status by western blot. A slightly lower ratio of total Phospho-

YAP/YAP was found in the $C2^{LN}$ MPM subgroup compared to the *NF2*-mutated MPM and other MPM (Fig. 3B and Supplementary Fig. S4C). All the MPM of the $C2^{LN}$ subgroup show a relative high percentage of nuclear YAP relative to total cell YAP in comparison to the other MPM (Supplementary Fig. S5A). The mRNA expressions of three YAP potential targeted genes (*CTGF* (connective tissue growth factor), *ANKRD1* (ankyrin repeat domain 1) and *CYR61* (cysteine-rich, angiogenic inducer, 61)) were also studied. We first verified that these three genes are YAP targeted genes in MPM by demonstrating that *CTGF*, *ANKRD1* and *CYR61* expressions were significantly decreased after *YAP1* knockdown by siRNA either in three MPM of the $C2^{LN}$ subgroup (MPM_08, MPM_40 and MPM_47) or in another MPM (MPM_32) (Supplementary Fig. S5B-C). *CTGF*, *ANKRD1* and *CYR61* expressions were then compared in 61 MPM in culture, including MPM of the $C2^{LN}$ subgroup, *NF2*-mutated MPM and other MPM. A slightly increased expression of these three genes was found in the $C2^{LN}$ MPM subgroup in subconfluent cells (Fig. 3C) and was enhanced when the cells were confluent (Supplementary Fig. S5D). Verteporfin, a potent YAP inhibitor, strongly inhibited cell viability in all MPM (Supplementary Fig. S5E). The MPM of the $C2^{LN}$ subgroup were more resistant to Verteporfin than other MPM (Supplementary Fig. S5F). Overall, these data suggest a high co-transcriptional activity of *YAP* and a low Hippo pathway activity in MPM of the $C2^{LN}$ subgroup.

MTOR phosphorylation and total protein expression were also analyzed by western blot (Fig. 3D-E and Supplementary Fig. S4C). RPPA data on mTOR phosphorylation were confirmed, suggesting that mTOR is less active in the $C2^{LN}$ MPM subgroup (Fig. 3D). A decrease in mTOR expression was also observed in the $C2^{LN}$ subgroup, indicating that lower phosphorylation of mTOR is linked to a lower protein expression (Fig. 3E).

Targeted treatment of the $C2^{LN}$ subgroup MPM

The low expression and phosphorylation of the mTOR protein allowed us to target mTOR in the $C2^{LN}$ MPM subgroup to determine whether mTOR inhibitors could affect cell viability. We selected a specific mTOR inhibitor (rapamycin) and an mTOR/PI3K/AKT inhibitor (PF_04691502). Treatment with rapamycin caused a slight decrease of cell viability in most of the cell lines, even at high concentrations (5-48% at 10 μM) (Supplementary Fig. S6A-B). In contrast, PF_04691502 significantly inhibited cell viability in all MPM (47-92% at 10 μM), but PF_04691502 sensitivity was variable between MPM in culture (Fig. 4A). Interestingly, the MPM of the $C2^{LN}$ subgroup were more sensitive to PF_04691502 than other MPM (Fig. 4A-B). Using two MPM of the $C2^{LN}$ subgroup, we confirmed that PF_04691502 inhibits mTOR by analyzing phosphorylation of mTOR downstream targets, 4E-BP1, p70 S6 kinase (P70-S6K) and S6 ribosomal protein (S6R) (Supplementary Fig. S6C). We used annexin V/propidium iodide staining assay to determine the PF_04691502 mechanism of cell death in two representative MPM. After treatment with gradient concentrations of PF_04691502, the apoptotic cells were increased from 13.2% to 85.4% in MPM of the $C2^{LN}$ subgroup (MPM_29) and from 12.9% to 24% in other MPM (MPM_17) (Fig. 4C-D).

Identification of *MOK*, a specific biomarker of the $C2^{LN}$ MPM subgroup

To define a specific biomarker the of $C2^{LN}$ MPM subgroup, we compared mRNA expression between the $C2^{LN}$ MPM subgroup and the other MPM using previously reported transcriptomic data (8) (Fig. 5A). A list of 42 deregulated genes was obtained with an adjusted *P*-value < 0.01 (Supplementary Table S5). We selected four upregulated genes (*MOK, CHRDL1, TXNRD2* and *PTPRB*) and one downregulated gene (*NEO1*), based on fold change and gene function. The mRNA expression level of these genes was further analyzed by qRT-PCR in all 61 MPM in culture. *MOK*, *CHRDL1*, *PTPRB* and *NEO1* showed highly significant deregulation in the $C2^{LN}$ MPM subgroup (Fig. 5B and Supplementary Fig. S7A). In si*LATS2* and/or si*NF2*-transfected MPM, only *MOK* (MAP overlapping kinase) mRNA was specifically upregulated after knocking down both *LATS2* and *NF2*, indicating that the *MOK*

gene is a potential biomarker of the $C2^{LN}$ MPM subgroup (Fig. 5C and Supplementary Fig. S7B). Furthermore, *MOK* mRNA expression was not modified by *YAP1* inhibition using specific siRNA in three MPM of the $C2^{LN}$ subgroup, suggesting that *MOK* expression was regulated by *LATS2*/*NF2* inactivation independently of YAP activity (Supplementary Fig. S7C). Moreover, we found a significant correlation between *MOK* mRNA expression and normalized AUC of PF_04691502-treated MPM cells, suggesting that *MOK* expression could also be a predictor of PF_04691502 sensitivity in MPM (Fig. 5D).

Discussion

Genetic alterations in members of the Hippo pathway are frequent in MPM cells. The most frequently mutated gene is *NF2,* an upstream regulator, with rates of 40 to 60% (20). Mutations in *LATS2* were first described by Murakami *et al*. (13) at a high rate of mutation (35% - 7/20 MPM in culture), which was not confirmed in two larger series of MPM tumor samples (4% - 2/53 MPM tumor samples; 3% - 6/202 tumor samples) (6, 14). In the Murakami series, 4/7 genetic alterations were large biallelic deletions (20% - 4/20 MPM in culture) and 3/7 were point mutations (15% - 3/20 MPM in culture). In the present larger series of 61 MPM cells in culture, a mutation rate of 11% of overall mutations (6% of point mutations and 5% of large deletions) was found. Large deletions represent 42% of overall mutations for *LATS2* in our series. Most sequencing methods do not make it possible to identify large biallelic deletions in tumor samples due to the presence of normal cells, in contrast to cell lines. Our sequencing data confirms that the point mutation rate of *LATS2* is around 5% in MPM and underlines the need to evaluate large biallelic deletions by FISH or other analyses to have a correct evaluation of *LATS2* genetic alterations in MPM tumor samples. Analysis of *LATS2* mRNA and protein expression in our MPM series suggests that genetic alterations are the main mechanism of inactivation for this gene. Genetic alterations of other Hippo pathway members have been described for *LATS1* (large tumor suppressor 1), *SAV1* (salvador homolog 1), *MST1*, *MST2* (macrophage stimulating 1 and 2), *RASSF1* (ras association domain family member 1) and *STK3* (serine/threonine kinase 3), but their mutation frequencies were very low (4, 6, 13, 14, 21). Since *LATS1* gene is a homolog of *LATS2*, we analyzed *LATS1* mRNA and protein expression by RT-qPCR and western blot respectively in our MPM series (data not shown). We observed similar mRNA expression of *LATS1*, but variable protein expression. Absence of LATS1 protein expression was observed in three of seven *LATS2*-mutated MPM and one of 34 wild-type MPM, showing a significant association (P=0.01) between *LATS2* gene mutation and LATS1 expression loss by a post-transcriptional mechanism. This observation needs to be confirmed in a larger series.

We identified co-occurring mutations of the two Hippo pathway members, *LATS2* and *NF2*, in 8% of MPM samples. It is generally expected that a single tumor has alterations in only one member of a given signal pathway. However, the discovery of an increasing number of mutated genes in human cancers has led to the identification of genes with co-occurring mutations, which mapped to the same pathway (22). *LATS2/NF2* co-occurring mutants were also found in the Murakami series of MPM in culture (15%), and in the Miyanaga (4%), Bott (2%) and Bueno (1%) tumor samples series (6, 13, 14, 21). These co-occurring mutations were more frequently detected in MPM in culture than in MPM tumor samples, consistent with the poor detection of large biallelic deletions in MPM tumor samples. Next generation sequencing (NGS) approaches are very efficient to detect variants, but may fail to identify large deletions because of the presence of contaminating normal stromal and immune cells in the tumor sample. Large deletions are common in MPM, *NF2* is also frequently altered by large exon biallelic deletion (59% in our series). An integrated approach is required to correctly estimate the frequency of *LATS2/NF2* co-occurring inactivation in tumor samples including multiplex ligation-dependent probe amplification (MLPA), fluorescence in situ hybridization (FISH) and immunohistochemistry. Data mining of DNA sequencing studies shows other co-occurring alterations in other Hippo pathway members, even they are infrequent in MPM (*LATS2/MST1*, *LATS2/RASSF1*, *LATS2/SAV1*, *NF2/LATS1*, *NF2/RASSF1*, *NF2/SAV1*) (6, 13, 14, 21). Furthermore, analysis of large-scale cancer genomics datasets of the cBioPortal database (http://www.cbioportal.org/, last access: November 16, 2016) did not identify other associations between *LATS2* and *NF2* gene mutations in other cancer types due to their low mutation frequencies. Consequently, *LATS2* and *NF2* co-occurring mutants seem to be relevant and specific to MPM carcinogenesis.

Additionally, we found that *LATS2/NF2* MPM mutants clustered in a specific $C2^{LN}$ subgroup of the C2 group, using the same clustering approach that led to the identification of the C1/C2 groups (8). Consequently, these mutants share a similar transcriptomic profile, suggesting a common mechanism of carcinogenesis. It is noteworthy that it is the first MPM

subgroup for which such a strong link between a mutation profile and gene expression signature is highlighted. We previously described a significant association between *BAP1* gene mutation and the C1 group (8), but unsupervised consensus classification of the C1 group did not distinguish *BAP1*-mutated MPM from *BAP1* wild-type MPM (data not shown). Furthermore, a recent clustering analysis based on transcriptomic data of large MPM tumor series did not reveal a strong association between gene mutations and transcriptomic clusters (6).

Two other MPM in culture (MPM_18 and MPM_38) are also present in the $C2^{LN}$ MPM subgroup. In MPM_18, the *LATS2* gene is altered by exon deletion, but no genetic alteration in *NF2* gene was identified and *NF2* expression was detected both at the mRNA and protein level (data not shown). Regulation of *NF2* in MPM may occur at different levels, including the post-translational mechanism. It was shown that *NF2* is rendered inactive by phosphorylation of Ser518 (23). This might be the case in MPM_18. MPM_38 has no mutation in *NF2* and *LATS2* genes, but show a strong overexpression of *WWTR1* that could support its presence in the $C2^{LN}$ MPM subgroup.

Our data suggest that co-inactivation of *LAST2* and *NF2* modulates MPM proliferation. *NF2* is a key gene of mesothelial carcinogenesis. Inactivation of *Nf2* in mice favored mesothelioma formation after exposure to asbestos, showing that it is driver gene of asbestos-induced mesothelial carcinogenesis (24). However, spontaneous mesothelioma is infrequent in *Nf2* homozygous conditional knockout mice, revealing that other genetic alterations are needed for MPM formation (25). It was shown that *NF2* re-expression inhibits invasiveness in two human mesothelioma cell lines (26), but inhibition by siRNA of *NF2* did not modify the invasion property of our MPM in culture *in vitro*. It was also shown that the re-expression of *NF2* or *LATS2* separately inhibited proliferation in MPM cell lines (13, 27). However, our data show that single inactivation of either *NF2 or LATS2* did not affect proliferation in three *NF2* wild-type MPM in culture. On the other hand, co-inactivation of

LAST2 and *NF2* led to a loss of contact inhibition, as shown by increased proliferation of siRNA knockdown cells at confluence and foci formation in *LATS2*/*NF2* MPM mutants. Loss of contact inhibition may promote tumor growth and is consistent with the worse prognosis of patients in the $C2^{LN}$ MPM subgroup compared to other MPM patients. Modeling of *LATS2* and *NF2* inactivation in mice would make it possible to better understand their contribution to MPM progression.

Identification of specific biomarkers of tumor subgroup, sharing similar molecular characteristic, is essential to select patients for target therapy. Gene expression based biomarkers are especially useful for molecular subgroups relying on various or complex genetic alterations, whose the identification by sequencing in tumor samples is problematic, such as the $C2^{LN}$ MPM subgroup. We identified the *MOK* gene as a specific biomarker overexpressed in the $C2^{LN}$ MPM subgroup. Unfortunately, we assayed several anti-MOK commercial antibodies, but none was able to accurately detect MOK protein expression. Nevertheless, analysis of gene expression on frozen tumors using RT-qPCR or on formalin-fixed paraffin-embedded tumors using multiplexed hybridization assay (NanoString nCounter system) should contribute to better identify patients with MPM tumors of the $C2^{LN}$ subgroup. Interestingly, *MOK* overexpression was also associated with poor prognosis in hepatocellular carcinoma patients (28). *MOK* overexpression is induced by the simultaneous siRNA knockdown of *LATS2* and *NF2* and not of *YAP1*, demonstrating that co-inactivation of *LATS2* and *NF2* leads to gene deregulation independently of YAP. *MOK* is a member of the MAP kinase family and considered as a tumor-associated antigen (RAGE-1) in renal carcinoma cells (29) and in some MPM (30). To date, the function of *MOK* in carcinogenesis remains largely unknown. *MOK* was found to decrease the cell invasive ability of hepatocellular carcinoma cells (28). We attempted to knockdown *MOK* expression using at least six different siRNAs from two different manufacturers. Unfortunately, *MOK* expression inhibition by siRNA was only partial and we were not able to evaluate its contribution to the proliferation and invasion of MPM cells.

In the present study, we identified specific signaling pathways deregulated in the $C2^{LN}$ MPM subgroup. As expected, we observed a decrease of Hippo signaling pathway activity (decrease of YAP phosphorylation and overexpression of *CTGF*, *CYR61* and *ANKRD1*, previously described (31, 32), and confirmed as YAP target genes by *YAP1* knockdown in MPM), not only in comparison to MPM without mutation in members of this pathway, but also in MPM with mutation solely in the *NF2* gene. Furthermore, the MPM of the $C2^{LN}$ subgroup were more resistant to Verteporfin, a potent YAP inhibitor, which disrupts YAP-TEAD interactions (33), than other MPM, consistent with higher YAP activity in the $C2^{LN}$ subgroup. It was previously suggested that MPM cells with *NF2* inactivation alone showed relatively modest YAP activation, and additional alterations of other molecules such as *SAV1*, *KIBRA*, *LATS1/2* and *AJUBA* lead to the enhancement of YAP activation (34). This hypothesis is supported by our data on *LATS2*/*NF2* MPM mutants and on *NF2* MPM mutants, which showed a heterogeneous mRNA expression of YAP target genes compared to the $C2^{LN}$ MPM subgroup

However, the Hippo pathway is not the only signaling pathway altered in the $C2^{LN}$ MPM subgroup. Our findings are consistent with a deregulation of mTOR in the $C2^{LN}$ MPM subgroup. MTOR is a serine/threonine kinase that belongs to the PI3K/AKT/mTOR signaling pathway and is often activated in MPM (20). It was suggested that the loss of merlin, encoded by the *NF2* gene, causes activation of mTOR signaling by studying 4E-BP1 and p70-S6-Kinase phosphorylation but not mTOR phosphorylation and expression (35). We analyzed, by western blot, the phosphorylation of 4E-BP1, p70-S6-Kinase and S6-Ribosomal-protein using the MPM panel of Supplementary Figure S4C (data not shown). We did not find significant difference in the phosphorylation level of these three proteins between the nine *NF2*-mutated MPM and the seven wild-type MPM. Our data show that mTOR phosphorylation is downregulated in the $C2^{LN}$ MPM subgroup. This downregulation is linked to a decrease of mTOR expression at the protein level, but not at the mRNA level. No difference was found in mRNA expression between the $C2^{LN}$ MPM subgroup and other MPM

in our transcriptomic data (data not shown). Little is currently known about mTOR post-translational regulation and protein degradation. MTOR is targeted for ubiquitination and proteasomal degradation by binding to the E3 ubiquitin ligase FBXW7 (F-box/WD repeat-containing protein 7) (36). Lysosomal degradation is another mechanism of mTOR protein expression regulation (37). Further studies are needed to understand the decrease of mTOR expression and, consequently, activity in the $C2^{LN}$ MPM subgroup.

In order to identify anticancer compounds specific to the $C2^{LN}$ subgroup of MPM, we then focused on mTOR inhibitors. Rapamycin, a specific mTOR inhibitor, showed a slight effect on MPM cell viability (inhibition of 20-30%). A previous study using this inhibitor on several MPM cell lines also revealed inhibition of cell growth up to only 30% after 48 h of treatment, except in one cell line (35). Furthermore, recent results of a phase II clinical trial showed that inhibition of mTOR alone by Everolimus (a rapamycin derivate) has a limited effect in MPM patients (38). The inefficiency of rapamycin could be explained by the activation of an AKT feedback after mTOR inactivation (39). In MPM, it was shown that rapamycin strongly inhibited mTOR activity in three MPM cell lines, but was associated with an increase of AKT activation (40). Dual inhibition of mTOR and PI3K/AKT seemed to be more efficient than single mTOR inhibition, with a significant effect on proliferation and survival of MPM cell lines, as recently described (41, 42). In agreement with these studies, PF_04691502, an mTOR/PI3K/AKT pathway inhibitor (43), strongly affected the viability of our MPM in culture. Furthermore, MPM of the $C2^{LN}$ subgroup were more sensitive than other MPM to PF_04691502 treatment. This result could be explained by the lower mTOR protein expression and activity in this subgroup, increasing the efficiency of this ATP-competitive dual inhibitor of mTOR and PI3K. PF_04691502 treatment affects cell viability in MPM and apoptotic cells were detected in MPM_29 and two other sensitive cell lines (data not shown). Our data suggest that induction of apoptosis by PF_04691502 contributes to affect cell viability in sensitive MPM in culture, as has been described in other tumor cell types (44). However, the plateau observed in cell viability at higher drug concentrations in most of the

MPM in culture also indicates contribution of growth arrest and autophagy. Interestingly, we found a correlation between *MOK* mRNA expression and PF_04691502 sensitivity, suggesting that *MOK* could be used as a biomarker of the $C2^{LN}$ MPM subgroup as well as of PF_04691502 sensitivity. PF_04691502 was already studied in phase I and phase II clinical trials for several advanced cancers and recurrent endometrial cancer (45, 46), which will facilitate the clinical transfer to MPM patients, especially to patients with *LATS2* and *NF2* mutations. Nevertheless, before considering a clinical transfer in MPM, the therapeutic value of PF_04691502 should be evaluated in preclinical animal models in relevant heterotopic and orthotopic xenograft models.

In conclusion, we clarified *LATS2* alterations in MPM and identified a specific MPM molecular subgroup, $C2^{LN}$, characterized by frequent co-occurring mutations in *LATS2* and *NF2*, two members of the Hippo signaling pathway. Patients of the $C2^{LN}$ subgroup had a poor survival prognosis, possibly in relation to a better propensity of tumor cells to grow independently of cell-cell contact inhibition. The Hippo signaling pathway and mTOR protein expression were altered in the $C2^{LN}$ MPM subgroup. This new subgroup is more sensitive to mTOR/PI3K/AKT pathway inhibitors. We identified the *MOK* gene as a potential biomarker of MPM patients of the $C2^{LN}$ subgroup and mTOR/PI3K/AKT pathway inhibitor sensitivity. Our data demonstrate the importance of combining molecular classification and genetic alterations to define a new molecular subgroup and a new potential therapeutic strategy.

References

1. Huang SX, Jaurand MC, Kamp DW, Whysner J, Hei TK. Role of mutagenicity in asbestos fiber-induced carcinogenicity and other diseases. J Toxicol Environ Health B Crit Rev. 2011;14:179-245.
2. Jean D, Daubriac J, Le Pimpec-Barthes F, Galateau-Salle F, Jaurand MC. Molecular changes in mesothelioma with an impact on prognosis and treatment. Arch Pathol Lab Med. 2012;136:277-93.
3. Jean D, Jaurand MC. Causes and pathophysiology of malignant pleural mesothelioma. Lung Cancer Management. 2015;4:10.
4. Guo G, Chmielecki J, Goparaju C, Heguy A, Dolgalev I, Carbone M, et al. Whole-exome sequencing reveals frequent genetic alterations in BAP1, NF2, CDKN2A, and CUL1 in malignant pleural mesothelioma. Cancer Res. 2015;75:264-9.
5. De Rienzo A, Archer MA, Yeap BY, Dao N, Sciaranghella D, Sideris AC, et al. Gender-Specific Molecular and Clinical Features underlie Malignant Pleural Mesothelioma. Cancer Res. 2015.
6. Bueno R, Stawiski EW, Goldstein LD, Durinck S, De Rienzo A, Modrusan Z, et al. Comprehensive genomic analysis of malignant pleural mesothelioma identifies recurrent mutations, gene fusions and splicing alterations. Nat Genet. 2016;48:407-16.
7. Tallet A, Nault JC, Renier A, Hysi I, Galateau-Salle F, Cazes A, et al. Overexpression and promoter mutation of the TERT gene in malignant pleural mesothelioma. Oncogene. 2014;33:3748-52.
8. de Reynies A, Jaurand MC, Renier A, Couchy G, Hysi I, Elarouci N, et al. Molecular Classification of Malignant Pleural Mesothelioma: Identification of a Poor Prognosis Subgroup Linked to the Epithelial-to-Mesenchymal Transition. Clin Cancer Res. 2014;20:1323–34.
9. Ehmer U, Sage J. Control of proliferation and cancer growth by the Hippo signaling pathway. Mol Cancer Res. 2015.
10. Yokoyama T, Osada H, Murakami H, Tatematsu Y, Taniguchi T, Kondo Y, et al. YAP1 is involved in mesothelioma development and negatively regulated by Merlin through phosphorylation. Carcinogenesis. 2008;29:2139-46.
11. Mizuno T, Murakami H, Fujii M, Ishiguro F, Tanaka I, Kondo Y, et al. YAP induces malignant mesothelioma cell proliferation by upregulating transcription of cell cycle-promoting genes. Oncogene. 2012;31:5117-22.
12. Felley-Bosco E, Stahel R. Hippo/YAP pathway for targeted therapy. Transl Lung Cancer Res. 2014;3:75-83.
13. Murakami H, Mizuno T, Taniguchi T, Fujii M, Ishiguro F, Fukui T, et al. LATS2 is a tumor suppressor gene of malignant mesothelioma. Cancer Res. 2011;71:873-83.
14. Bott M, Brevet M, Taylor BS, Shimizu S, Ito T, Wang L, et al. The nuclear deubiquitinase BAP1 is commonly inactivated by somatic mutations and 3p21.1 losses in malignant pleural mesothelioma. Nat Genet. 2011;43:668-72.
15. Jean D, Thomas E, Manie E, Renier A, de Reynies A, Lecomte C, et al. Syntenic Relationships between Genomic Profiles of Fiber-Induced Murine and Human Malignant Mesothelioma. Am J Pathol. 2011;178:881-94.
16. Andujar P, Pairon JC, Renier A, Descatha A, Hysi I, Abd-Alsamad I, et al. Differential mutation profiles and similar intronic TP53 polymorphisms in asbestos-related lung cancer and pleural mesothelioma. Mutagenesis. 2013;28:323-31.
17. Rondeau S, Vacher S, De Koning L, Briaux A, Schnitzler A, Chemlali W, et al. ATM has a major role in the double-strand break repair pathway dysregulation in sporadic breast carcinomas and is an independent prognostic marker at both mRNA and protein levels. Br J Cancer. 2015;112:1059-66.
18. Troncale S, Barbet A, Coulibaly L, Henry E, He B, Barillot E, et al. NormaCurve: a SuperCurve-based method that simultaneously quantifies and normalizes reverse phase protein array data. PLoS One. 2012;7:e38686.

19. Ritchie ME, Phipson B, Wu D, Hu Y, Law CW, Shi W, et al. limma powers differential expression analyses for RNA-sequencing and microarray studies. Nucleic Acids Res. 2015;43:e47.
20. Jaurand MC, Jean D. Biomolecular Pathways and Malignant Pleural Mesothelioma. In: Mineo CT, editor. Malignant Pleural Mesothelioma: Present Status and Future Directions: Bentham eBooks; 2016. p. 169-92.
21. Miyanaga A, Masuda M, Tsuta K, Kawasaki K, Nakamura Y, Sakuma T, et al. Hippo pathway gene mutations in malignant mesothelioma: revealed by RNA and targeted exon sequencing. J Thorac Oncol. 2015;10:844-51.
22. Cui Q. A network of cancer genes with co-occurring and anti-co-occurring mutations. PLoS One. 2010;5.
23. Thurneysen C, Opitz I, Kurtz S, Weder W, Stahel RA, Felley-Bosco E. Functional inactivation of NF2/merlin in human mesothelioma. Lung Cancer. 2009;64:140-7.
24. Fleury-Feith J, Lecomte C, Renier A, Matrat M, Kheuang L, Abramowski V, et al. Hemizygosity of Nf2 is associated with increased susceptibility to asbestos-induced peritoneal tumours. Oncogene. 2003;22:3799-805.
25. Jongsma J, van Montfort E, Vooijs M, Zevenhoven J, Krimpenfort P, van der Valk M, et al. A conditional mouse model for malignant mesothelioma. Cancer Cell. 2008;13:261-71.
26. Poulikakos PI, Xiao GH, Gallagher R, Jablonski S, Jhanwar SC, Testa JR. Re-expression of the tumor suppressor NF2/merlin inhibits invasiveness in mesothelioma cells and negatively regulates FAK. Oncogene. 2006;25:5960-8.
27. Xiao GH, Gallagher R, Shetler J, Skele K, Altomare DA, Pestell RG, et al. The NF2 tumor suppressor gene product, merlin, inhibits cell proliferation and cell cycle progression by repressing cyclin D1 expression. Mol Cell Biol. 2005;25:2384-94.
28. Cha HJ, Kim J, Hong SM, Hong SJ, Park JH, Kim ES, et al. Overexpression of renal tumor antigen is associated with tumor invasion and poor prognosis of hepatocellular carcinoma. Ann Surg Oncol. 2012;19 Suppl 3:S404-11.
29. Neumann E, Engelsberg A, Decker J, Storkel S, Jaeger E, Huber C, et al. Heterogeneous expression of the tumor-associated antigens RAGE-1, PRAME, and glycoprotein 75 in human renal cell carcinoma: candidates for T-cell-based immunotherapies? Cancer Res. 1998;58:4090-5.
30. Sigalotti L, Coral S, Altomonte M, Natali L, Gaudino G, Cacciotti P, et al. Cancer testis antigens expression in mesothelioma: role of DNA methylation and bioimmunotherapeutic implications. Br J Cancer. 2002;86:979-82.
31. Zhao B, Ye X, Yu J, Li L, Li W, Li S, et al. TEAD mediates YAP-dependent gene induction and growth control. Genes Dev. 2008;22:1962-71.
32. Stein C, Bardet AF, Roma G, Bergling S, Clay I, Ruchti A, et al. YAP1 Exerts Its Transcriptional Control via TEAD-Mediated Activation of Enhancers. PLoS Genet. 2015;11:e1005465.
33. Liu-Chittenden Y, Huang B, Shim JS, Chen Q, Lee SJ, Anders RA, et al. Genetic and pharmacological disruption of the TEAD-YAP complex suppresses the oncogenic activity of YAP. Genes Dev. 2012;26:1300-5.
34. Tanaka I, Osada H, Fujii M, Fukatsu A, Hida T, Horio Y, et al. LIM-domain protein AJUBA suppresses malignant mesothelioma cell proliferation via Hippo signaling cascade. Oncogene. 2015;34:73-83.
35. Lopez-Lago MA, Okada T, Murillo MM, Socci N, Giancotti FG. Loss of the tumor suppressor gene NF2, encoding merlin, constitutively activates integrin-dependent mTORC1 signaling. Mol Cell Biol. 2009;29:4235-49.
36. Mao JH, Kim IJ, Wu D, Climent J, Kang HC, DelRosario R, et al. FBXW7 targets mTOR for degradation and cooperates with PTEN in tumor suppression. Science. 2008;321:1499-502.

37. Hu Y, Carraro-Lacroix LR, Wang A, Owen C, Bajenova E, Corey PN, et al. Lysosomal pH Plays a Key Role in Regulation of mTOR Activity in Osteoclasts. J Cell Biochem. 2016;117:413-25.
38. Ou SH, Moon J, Garland LL, Mack PC, Testa JR, Tsao AS, et al. SWOG S0722: phase II study of mTOR inhibitor everolimus (RAD001) in advanced malignant pleural mesothelioma (MPM). J Thorac Oncol. 2015;10:387-91.
39. Carracedo A, Ma L, Teruya-Feldstein J, Rojo F, Salmena L, Alimonti A, et al. Inhibition of mTORC1 leads to MAPK pathway activation through a PI3K-dependent feedback loop in human cancer. J Clin Invest. 2008;118:3065-74.
40. Barbone D, Yang TM, Morgan JR, Gaudino G, Broaddus VC. Mammalian target of rapamycin contributes to the acquired apoptotic resistance of human mesothelioma multicellular spheroids. J Biol Chem. 2008;283:13021-30.
41. Zhou S, Liu L, Li H, Eilers G, Kuang Y, Shi S, et al. Multipoint targeting of the PI3K/mTOR pathway in mesothelioma. Br J Cancer. 2014;110:2479-88.
42. Echeverry N, Ziltener G, Barbone D, Weder W, Stahel RA, Broaddus VC, et al. Inhibition of autophagy sensitizes malignant pleural mesothelioma cells to dual PI3K/mTOR inhibitors. Cell Death Dis. 2015;6:e1757.
43. Cheng H, Bagrodia S, Bailey S, Edwards M, Hoffman J, Hu Q, et al. Discovery of the highly potent PI3K/mTOR dual inhibitor PF-04691502 through structure based drug design. Med Chem Commun. 2010;1:139-44.
44. Wang FZ, Peng J, Yang NN, Chuang Y, Zhao YL, Liu QQ, et al. PF-04691502 triggers cell cycle arrest, apoptosis and inhibits the angiogenesis in hepatocellular carcinoma cells. Toxicol Lett. 2013;220:150-6.
45. Britten CD, Adjei AA, Millham R, Houk BE, Borzillo G, Pierce K, et al. Phase I study of PF-04691502, a small-molecule, oral, dual inhibitor of PI3K and mTOR, in patients with advanced cancer. Invest New Drugs. 2014;32:510-7.
46. Del Campo JM, Birrer M, Davis C, Fujiwara K, Gollerkeri A, Gore M, et al. A randomized phase II non-comparative study of PF-04691502 and gedatolisib (PF-05212384) in patients with recurrent endometrial cancer. Gynecol Oncol. 2016.

Table

Table 1. Clinico-pathological and molecular characteristics of MPM.

	MPM cells in culture (*n* = 61)
Gender, *n* (%)	
Male	48 (79)
Female	13 (21)
Age (years)	
Median ± SD	65 ± 10
Range	37 - 89
Histology, *n* (%)	
Epithelioid	43 (74)
Biphasic	8 (14)
Sarcomatoid	6 (10)
Desmoplastic	1 (2)
Asbestos exposure, *n* (%)	
Exposed	47 (80)
Non-exposed	12 (20)
Survival (months)	
Median	10
Range	0.3 - 118.8
Molecular Group, *n* (%)	
C1	20 (33)
C2	41 (67)
Genetic alterations, *n* (%)	
CDKN2A	46 (75)
CDKN2B	41 (67)
BAP1	30 (49)
NF2	27 (44)
TP53	6 (10)

MPM, malignant pleural mesothelioma.

Legends of figures

Figure 1. *LATS2* alterations in MPM cells in culture

A, Schematic representation of the *LATS2* gene with genetic alterations characterized by Sanger sequencing. Large exon deletions are shown at the bottom. **B**, *LATS2* mRNA expression was measured by qRT-PCR. Dot plots of -ΔΔCt values are shown for wild type (black), mutated (blue) and exon-deleted MPM (red). **C**, Cell extracts from wild-type and *LATS2* MPM mutants were analyzed by western blot using anti-LATS2 antibody. α-tubulin expression was used as a control. wt: wild type; mut: mutated; del: deletion. **D**, Heatmap representation of genetic alteration profile of MPM in culture (n=61) for *CDKN2A*, *CDKN2B*, *BAP1*, *NF2*, *LATS2* and *TP53* genes. Dark blue is for exon deletions and light blue for point mutations. The MPM molecular classification is shown at the bottom: C1 group (green) and C2 group (red).

Figure 2. Characteristics of the $C2^{LN}$ MPM subgroup and effect of *LATS2*/*NF2* inactivation on MPM proliferation

A, Hierarchical unsupervised consensus classification of 23 MPM in culture from the C2 group was performed on gene expression profiles. The consensus dendrogram is shown. The three *LATS2/NF2* co-mutants (bold black line) are included in a specific subgroup referred to as $C2^{LN}$. **B**, Differences between overall survival of the *LATS2/NF2* wild-type MPM, *NF2* MPM mutants and the $C2^{LN}$ MPM subgroup are shown. The Logrank test *P*-value is indicated. **C**, One *LATS2/NF2* wild-type MPM (MPM_34) was transfected with siControl or both si*LATS2* and si*NF2*. Proliferation was followed by MTS assay for 120 hours. Results are expressed as the mean ± SEM of one representative experiment. **D**, Three *LATS2/NF2* wild-type MPM were transfected with siControl, si*LATS2*, si*NF2* or both si*LATS2* and si*NF2*. Two

different siRNAs for each targeted gene were used. Proliferation was quantified by MTS assay 96 hours after siRNA transfection. The mean of the two different siRNAs for each targeted genes was calculated and compared to an untransfected control. The histogram shows fold changes ± SD of one representative experiment. Statistical comparisons were performed on two or more independent experiments compared to siControl.

Figure 3. Signaling pathway activation in the $C2^{LN}$ MPM subgroup

A, RPPA analysis was performed on cell extracts of 39 MPM using antibodies specific to 40 phosphorylated proteins, key members of several major signaling pathways. The volcanoplot of RPPA data comparing the $C2^{LN}$ MPM subgroup to other MPM is shown. **B, D-E,** Cell extracts from the $C2^{LN}$ MPM subgroup, *NF2* MPM mutants and other MPM were analyzed by western blot. The boxplot shows the Phospho-YAP/YAP ratio (**B**) and Phospho-mTOR and mTOR ratios normalized to α-tubulin (**D-E**) determined from western blot signal intensity. **C**, mRNA expressions of Hippo pathway target genes (*CTGF*, *ANKRD1* and *CYR61*) were measured by qRT-PCR. Dot plots of -ΔΔCt values are shown for the $C2^{LN}$ MPM subgroup, *NF2* MPM mutants and other MPM. Statistical comparisons were performed by comparing the $C2^{LN}$ MPM subgroup to *NF2* MPM mutants and other MPM.

Figure 4. Effect of mTOR/PI3K/AKT inhibitor on cell viability

A, Cell viability curves of 18 MPM were determined in the presence of a gradient concentration of PF_04691502, a mTOR/PI3K/AKT inhibitor. Each point represents the mean ± SD of two independent experiments. **B,** PF_04691502-normalized AUCs of each MPM are compared between the $C2^{LN}$ MPM subgroup and other MPM. **C-D**, One MPM of the $C2^{LN}$ subgroup (MPM_29) and another MPM (MPM_17) were treated with gradient concentration of PF_04691502 for 48 h. MPM cells were stained with Annexin V-Alexa Fluor 488 and

propidium iodide. Early apoptosis, late apoptosis and necrosis were determined using flow cytometry (**C**). The percentage of cells in the lower left quadrant (live cells), the lower right quadrant (early apoptotic cells), the upper right quadrant (late apoptotic cells) and the upper left quadrant (necrotic cells) was quantified at a gradient concentration of PF_04691502 (**D**). Results are shown for one representative experiment.

Figure 5. Identification of a $C2^{LN}$ MPM subgroup biomarker

A, Diagram of selection, from transcriptomic data, of deregulated genes between the $C2^{LN}$ MPM subgroup and other MPM. **B-C**, *MOK* mRNA expressions were measured by qRT-PCR. Dot plots of -ΔΔCt values are shown for the $C2^{LN}$ MPM subgroup and the other MPM. Open circles and open squares represent MPM included in transcriptomic analysis; closed circles and closed squares represent MPM not included in transcriptomic analysis (**B**). Three *LATS2/NF2* wild-type MPM were transfected with siControl, si*LATS2*, si*NF2* or both si*LATS2* and si*NF2*. Two different siRNAs for each targeted gene were used. The mean of $2^{-\Delta\Delta Ct}$ obtained from the two different siRNAs of each targeted gene was calculated. The histogram shows the mean ± SD of one representative experiment. Statistical comparisons were performed on two or more independent experiments compared to siControl (**C**). **D**, Correlation between *MOK* mRNA expression and PF_04691502-normalized AUCs of 18 MPM in culture. Each point represents the mean ± SD of two independent experiments. Circle: other MPM; Square: $C2^{LN}$ MPM subgroup.

Figure 1

A

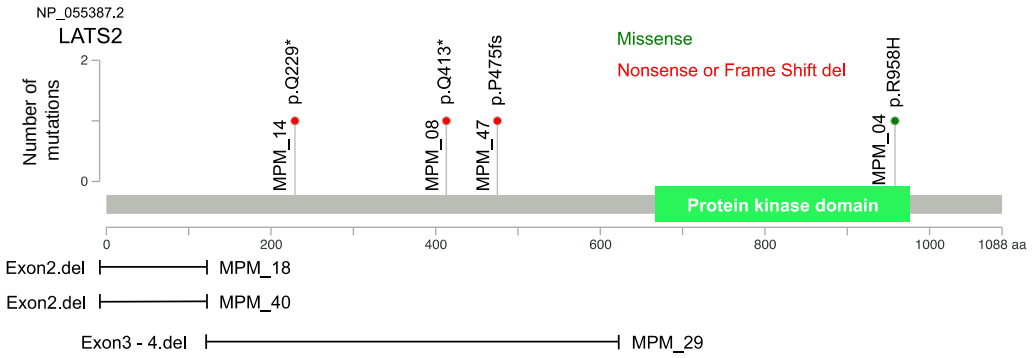

B

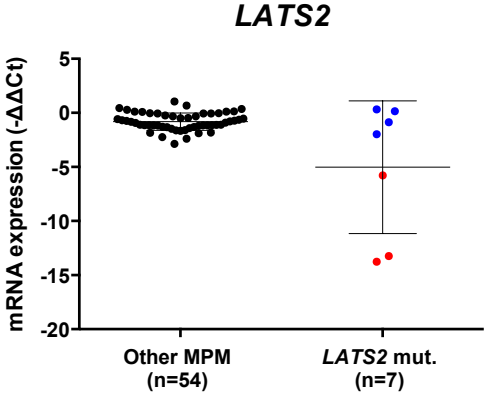

C

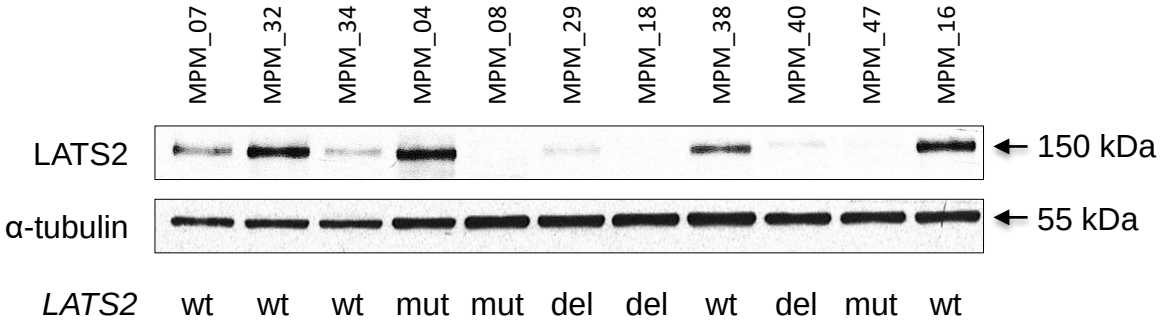

D

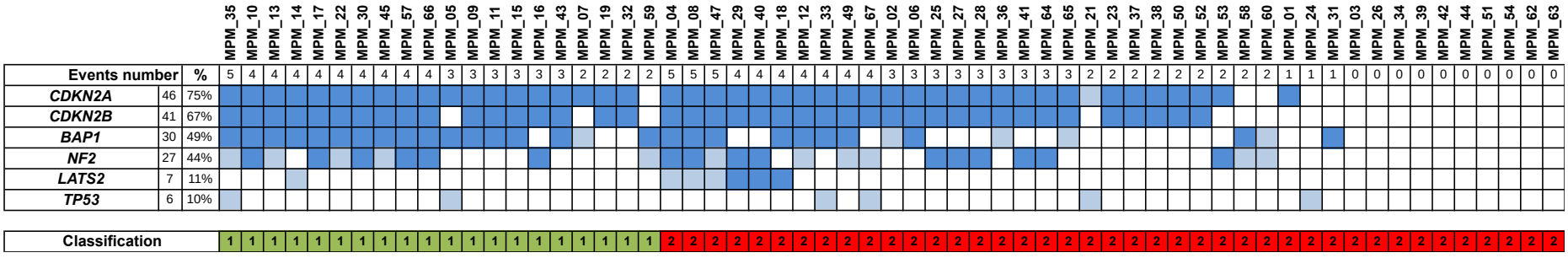

Figure 2

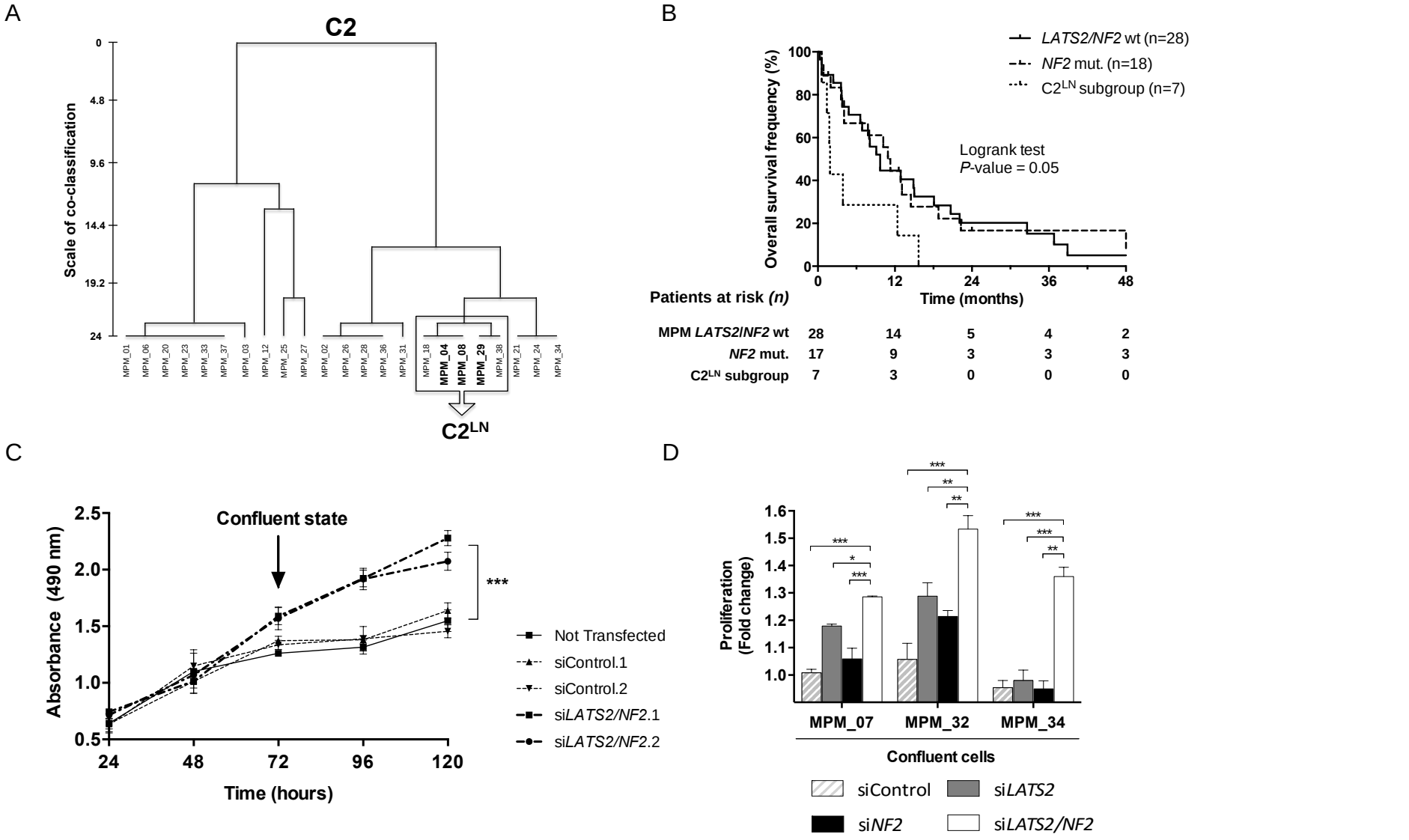
A
C2
Scale of co-classification
0
4.8
9.6
14.4
19.2
24
MPM_01
MPM_06
MPM_20
MPM_23
MPM_33
MPM_37
MPM_03
MPM_12
MPM_25
MPM_27
MPM_02
MPM_26
MPM_28
MPM_36
MPM_31
MPM_18
MPM_04
MPM_08
MPM_29
MPM_38
MPM_21
MPM_24
MPM_34
C2LN
B
LATS2/NF2 wt (n=28)
NF2 mut. (n=18)
C2LN subgroup (n=7)
Overall survival frequency (%)
100
80
60
40
20
0
Logrank test
P-value = 0.05
0
12
24
36
48
Time (months)
Patients at risk (n)
MPM LATS2/NF2 wt 28 14 5 4 2
NF2 mut. 17 9 3 3 3
C2LN subgroup 7 3 0 0 0
C
Confluent state
Absorbance (490 nm)
2.5
2.0
1.5
1.0
0.5
***
24
48
72
96
120
Time (hours)
Not Transfected
siControl.1
siControl.2
siLATS2/NF2.1
siLATS2/NF2.2
D
Proliferation (Fold change)
1.6
1.5
1.4
1.3
1.2
1.1
1.0
***
*
***
***
**
**
***
***
**
MPM_07
MPM_32
MPM_34
Confluent cells
siControl
siLATS2
siNF2
siLATS2/NF2

Figure 3

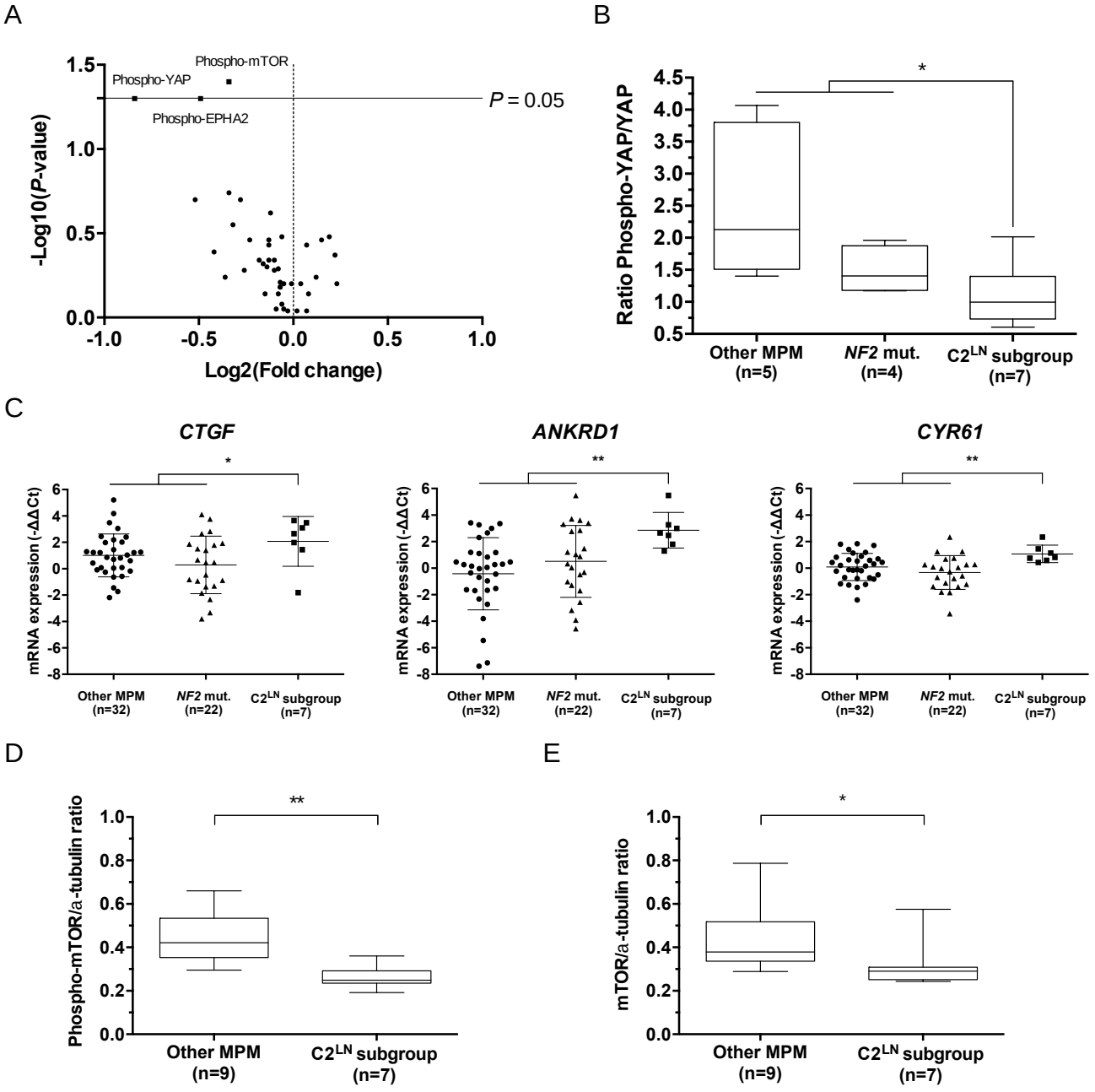
A
Phospho-mTOR
Phospho-YAP
Phospho-EPHA2
P = 0.05
-Log10(P-value)
Log2(Fold change)
B
Ratio Phospho-YAP/YAP
Other MPM (n=5)
NF2 mut. (n=4)
C2LN subgroup (n=7)
C
CTGF
ANKRD1
CYR61
mRNA expression (-ΔΔCt)
Other MPM (n=32)
NF2 mut. (n=22)
C2LN subgroup (n=7)
D
Phospho-mTOR/a-tubulin ratio
Other MPM (n=9)
C2LN subgroup (n=7)
E
mTOR/a-tubulin ratio
Other MPM (n=9)
C2LN subgroup (n=7)

Figure 4

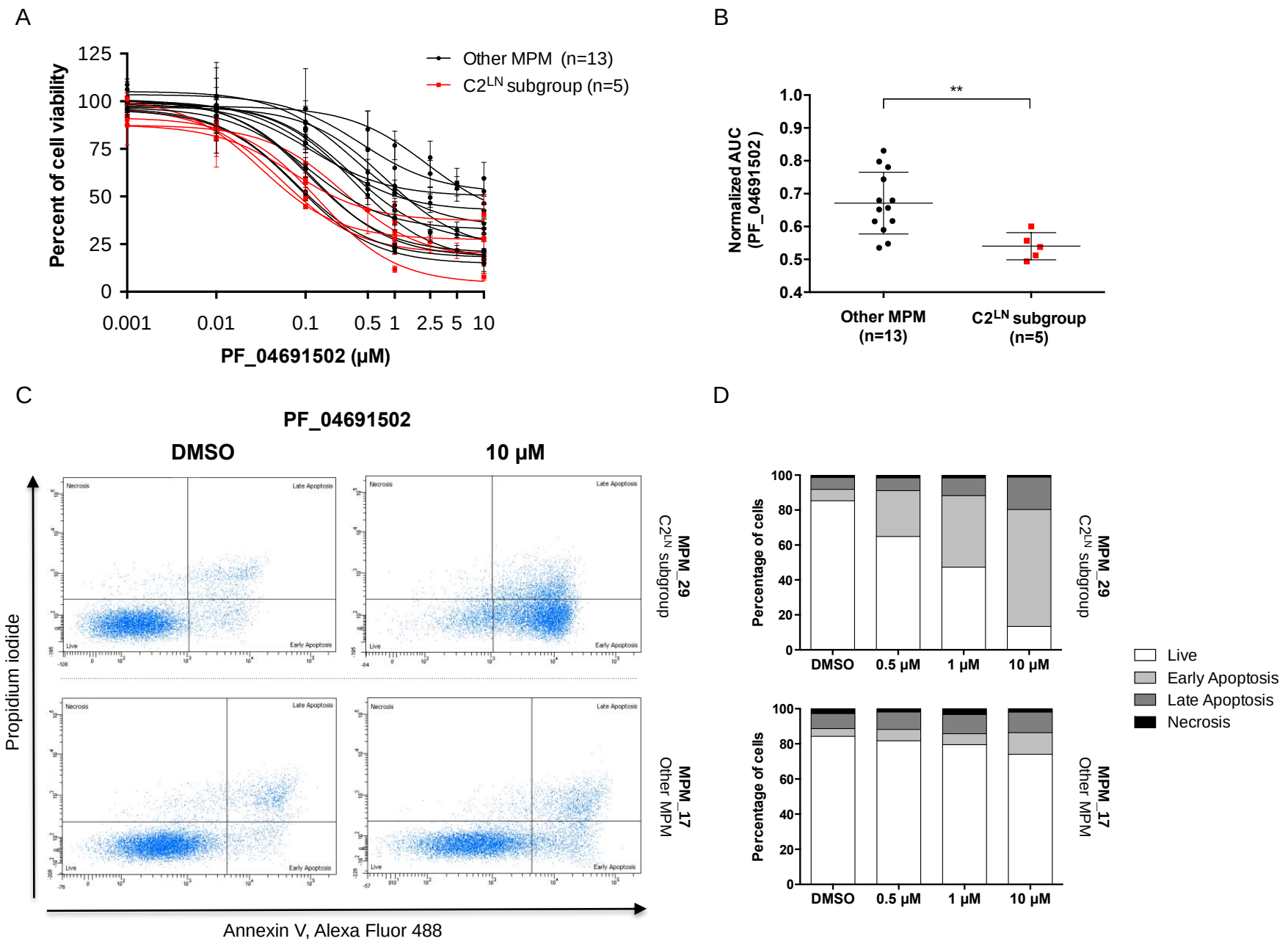
A
Percent of cell viability
125
100
75
50
25
0
0.001
0.01
0.1
0.5 1
2.5 5
10
PF_04691502 (µM)
Other MPM (n=13)
C2LN subgroup (n=5)
B
Normalized AUC (PF_04691502)
1.0
0.9
0.8
0.7
0.6
0.5
0.4
**
Other MPM (n=13)
C2LN subgroup (n=5)
C
PF_04691502
DMSO
10 µM
Propidium iodide
Annexin V, Alexa Fluor 488
Necrosis
Late Apoptosis
Live
Early Apoptosis
MPM_29
C2LN Subgroup
MPM_17
Other MPM
D
Percentage of cells
100
80
60
40
20
0
DMSO
0.5 µM
1 µM
10 µM
MPM_29
C2LN Subgroup
MPM_17
Other MPM
Live
Early Apoptosis
Late Apoptosis
Necrosis

Figure 5

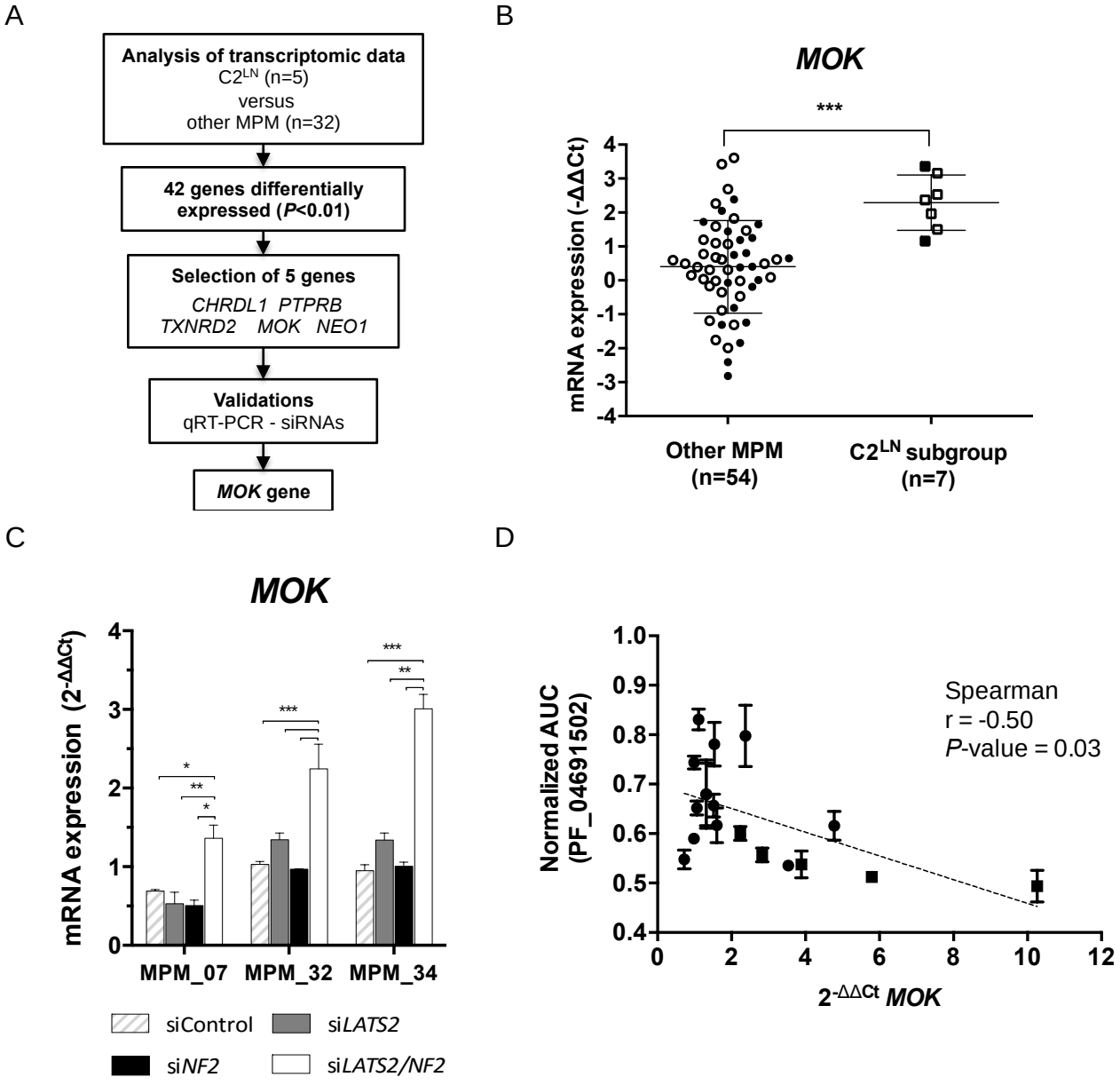
A
Analysis of transcriptomic data
C2LN (n=5)
versus
other MPM (n=32)
42 genes differentially expressed (P<0.01)
Selection of 5 genes
CHRDL1 PTPRB
TXNRD2 MOK NEO1
Validations
qRT-PCR - siRNAs
MOK gene
B
MOK
***
mRNA expression (-ΔΔCt)
Other MPM (n=54)
C2LN subgroup (n=7)
C
MOK
mRNA expression (2-ΔΔCt)
MPM_07
MPM_32
MPM_34
siControl
siLATS2
siNF2
siLATS2/NF2
D
Normalized AUC (PF_04691502)
Spearman
r = -0.50
P-value = 0.03
2-ΔΔCt MOK